Cauda equina repair in the rat: Part 3. Axonal regeneration across Schwann cell seeded collagen foam

Samuel J. Mackenzie, MD, PhD[1], **Juneyoung L. Yi, MD**[2], **Amit Singla, MD**[2], **Thomas M. Russell, BS**[3], **Donna J. Osterhout, PhD**[3], and **Blair Calancie, PhD**[2]

[1]Department of Neuroscience, Upstate Medical University, Syracuse, NY, 13210

[2]Department of Neurosurgery, Upstate Medical University, Syracuse, NY, 13210

[3]Department of Cell and Developmental Biology, Upstate Medical University, Syracuse, NY, 13210

Abstract

Introduction—Treatments for patients with cauda equina injury are limited.

Methods—In this study, we first used retrograde labeling to determine the relative contributions of cauda equina motor neurons to intrinsic and extrinsic rat tail muscles. Next, we transected cauda equina ventral roots and proceeded to bridge the proximal and distal stumps with either a type I collagen scaffold coated in laminin (CL) or a collagen-laminin scaffold that was also seeded with Schwann cells (CLSC). Regeneration was assessed by way of serial retrograde labeling.

Results—After accounting for the axonal contributions to intrinsic vs extrinsic tail muscles, we noted a higher degree of double labeling in the CLSC group ($58.0 \pm 39.6\%$) as compared to the CL group ($27.8 \pm 16.0\%$; $p = 0.02$), but not the control group ($33.5 \pm 18.2\%$; $p = 0.10$).

Discussion—Our findings demonstrate the feasibility of using Schwann cell seeded collagen-laminin scaffolds in cauda equina injury repair.

Keywords

cauda equina; motor neurons; regeneration; retrograde labeling; Schwann cells

Introduction

Traumatic injury to the cauda equina results in a devastating clinical syndrome for patients and presents a formidable challenge to the physicians charged with treating it.[1,2] The spontaneous regeneration of injured axons is dependent upon the degree of crush at the injury site and, in the event that the nerve root has undergone a loss of continuity, the extent of the gap between proximal and distal nerve root stumps.[3,4] Intradural repair allows the surgeon to minimize the injury site gap, optimize the alignment of proximal and distal stumps, and manipulate the environment at the lesion into one more conducive to axonal

regeneration through the implantation of grafts, scaffolds, anti-scarring compounds, or other growth-promoting agents. However, given the prognostic uncertainty that surrounds many cauda equina injuries and the paucity of established treatments, attempts at intradural repair of injured nerve roots are exceptionally rare.[5,6] A more common approach involves spinal stabilization and decompression of the canal space.[7–11] With the poor prognosis for spontaneous recovery of neurologic function, intradural repair of nerve roots could become a clinical option in more severe cases of cauda equina injury, provided that technical and surgical barriers can be overcome.

To this end, our laboratory has been working toward a treatment paradigm using a novel rat model of cauda equina injury.[12–14] In this study, we describe the relative axonal contributions to intrinsic and extrinsic tail muscles, identify regenerating axons innervating the intrinsic tail muscles, and examine the stimulatory effect of scaffolds on axonal regrowth after cauda equina injury.

Materials and Methods

Experiment 1: Motor neuron targets and counts

Surgical procedures and serial retrograde labeling—All experimental protocols described in this paper were approved by the Animal Care and Use Committee of Upstate Medical University, following the guidelines and provisions of the Association for Assessment and Accreditation of Laboratory Animal Care. Eight adult female Fischer 344/ DuCl rats (3 – 5 months age; Charles River; Hamilton, MA) were used in the first experiment.

Detailed surgical methods are described in the Supplemental Material section. Supplemental Figure 1 is a schematic depiction of the serial retrograde labeling for motor neuron localization. For caudales nerve labeling, the dorsal caudales nerve (DCN), which runs medially to the extensor caudae lateralis muscle, was exposed and cut, and the proximal stump was bathed for 10 minutes in a small foil container filled with Gelfoam soaked in True Blue (TB; Invitrogen) retrograde tracer. The ventral caudales nerve (VCN) was exposed at the same vertebral level by dissecting between the transverse processes of the coccygeal vertebrae and gently pulling the nerve through the opening with a small hook. The VCN was cut and labeled with TB as previously described. The entire procedure was repeated on the opposite side such that all four caudales nerves were transected and labeled with TB.

One week after the caudales nerve labeling, single ventral roots were labeled in the same animals. The general protocol used to identify and transect cauda equina ventral roots has been described previously[12], and is outlined in the Supplemental Materials section. Once a ventral root was identified, it was cut. The proximal stump of the transected nerve root was bathed for 10 minutes in a small foil container filled with Gelfoam soaked in fluoro-ruby (FR; Invitrogen; N=8). In some animals, we identified and labeled a second ventral root with fluoro-emerald (FE; Invitrogen; N=4) to increase the number of ventral roots labeled.

Tissue processing and microscopy—One week after ventral root labeling, rats were sacrificed and transcardially perfused with saline followed by paraformaldehyde. Spinal cords were dissected out, placed in 10% sucrose for cryoprotection, and embedded in OCT compound. The entire width of the caudal spinal cord was serially sectioned from dorsal to ventral in longitudinal serial frozen sections (from T12 and below; 50 μm thick), mounted onto glass slides, washed in PBS, and coverslipped using Prolong Gold antifade reagent.

Images of fluorescently labeled sections and neuronal somata were captured using a Zeiss Axio Imager A.1 microscope (Carl Zeiss, Germany) with standard fluorescent filters, a Zeiss AxioCam MRm camera (Carl Zeiss, Germany), and Axiovision software (Version 4.8.2.0, Carl Zeiss Microimaging). Labeled somata were counted on every serial section, allowing for an examination of the entire caudal spinal cord for each animal. Cells were not counted unless there was a full cell profile with a nucleus visible; fragments of cells were not counted (additional details in Supplemental Materials).[15]

Data analysis—Variables of interest included the number of single labeled cells, FR+ or FE+, and the number of double labeled cells (i.e., FR+TB+ or FE+TB+) observed in the ventral horn of the spinal cord. The percentage of double labeled motor neurons was calculated by multiplying ratios of double labeled cells to total FR+ or FE+ cells by 100. All data are presented as mean ± standard deviation.

Experiment 2: Axonal repair and regeneration

Schwann cell isolation—Schwann cells were isolated from the sciatic nerve explants from three-day-old Fischer 344/DuCl rat pups (N=20 from two litters; Charles River; Wilmington, MA) and purified to at least 97% purity prior to implantation, as determined by S-100 and Krox 20 labeling combined with DAPI (Supplemental Figure 2 showing Krox 20 + DAPI). Schwann cells were seeded onto the collagen-laminin scaffolds and used in the repair of a subset of animals (CLSC) immediately after transecting a ventral root and labeling it with TB.

Collagen-laminin scaffolds—Bovine type I collagen foam (ACE Surgical Supply, Inc., Brockton, MA) was cut into 3mm × 3mm × 3mm segments (henceforth referred to as scaffolds) and kept in dilute laminin for 24 hours. Schwann cells (200,000 of purified cells) were added to each scaffold (referred to as *seeded*); scaffolds without cells (*unseeded*) were used as controls. Seeded and unseeded scaffolds were incubated in Schwann cell culture media for two days, after which they were washed three times in PBS prior to implantation. Successful attachment of Schwann cells was confirmed in a subset of scaffolds by DAPI labeling of cell nuclei present in the scaffold (data not shown). Schwann cell death was not formally assessed, though no chromosomal condensation or nuclear shape change suggestive of apoptosis was noted on scaffold imaging.

Ventral root labeling and repair—The basic experimental paradigm used in this experiment is depicted in Supplemental Figure 3. Twenty adult female Fischer 344/DuCl rats (3 – 5 months age; Charles River; Hamilton, MA) were used. The protocol used to identify and transect cauda equina ventral roots was the same as that described above.

Following transection, the proximal stump of the transected nerve root was bathed for 10 minutes in a small foil container filled with Gelfoam soaked in True Blue (TB; Invitrogen) retrograde tracer. The distal stump was turned perpendicularly to one side of the nerve root, so we could easily find it prior to repair.

Nerve root repair was not performed in the injury control group (group NR; N=8). For the experimental groups, the repair procedure involved placing a Schwann cell seeded (group CLSC, N=6) or unseeded (group CL, N=6) scaffold into the lesion site, such that the scaffold bridged a 3 mm gap between the ends of the distal and proximal stumps. The perineurium of each stump was tacked to either end of the scaffold with fibrin glue.

Retrograde labeling of caudales nerves—Eight weeks after the initial injury and repair, the caudales nerves were surgically exposed one at a time at the base of the tail, cut, and bathed in fluoro-ruby tracer (FR; Invitrogen) as previously described. Axons that regenerated across the injury site and through the caudales nerves to the tail base would be double labeled with both TB and FR, while non-regenerated neurons would only be labeled with TB (Supplemental Figure 3A). This double labeling approach has been used to confirm regeneration in a number of peripheral nerve injury studies.[16–18]

Animal sacrifice and tissue processing—One week after FR labeling, rats were sacrificed and transcardially perfused with saline and paraformaldehyde. Spinal cords were dissected out, placed in 10% sucrose, and refrigerated for at least 48 hours before being embedded and frozen in OCT compound. Longitudinal or cross-sectional serial sections of 50 μm were mounted onto glass slides, washed in PBS, and coverslipped using Prolong Gold antifade reagent prior to microscopy.

Data analysis—Images of fluorescently labeled sections and cells were captured as described above. Cell counts were performed by two blinded, independent investigators who were not informed of the treatment group. A cell was considered double labeled if it showed co-localization of FR and TB. As in the first experiment, the total number of cells counted was halved for each animal per the Abercrombie method (Supplemental Material), and this number was used in our analysis under the conservative assumption that, on average, each cell would be visible on two adjacent serial sections.

The percentage of double labeled cells in each group was calculated by dividing the number of double labeled cells by the number of TB+ cells and averaging these results across animals. Since the axons of the labeled somata could feasibly take one of two possible trajectories prior to the Fluoro-ruby labeling point (i.e., extrinsic-bound or intrinsic-bound), we also used the upper bound of this estimate of intrinsic-bound motor neurons to calculate a corrected percentage of double labeled cells (i.e., the percentage of double labeled cells divided by the ratio of intrinsic-bound motor neurons). Retrograde labeling data were compared across groups using one-way ANOVA with Tukey's post hoc tests for multiple pairwise comparisons. All data are presented as mean ± standard deviation.

Results

1: Motor neuron targets and counts

Motor neuron localization—There were 399 ± 206 motor neurons labeled with TB following exposure of their axons within the caudales nerve at the base of the tail. These motor neurons innervated intrinsic tail muscles, thereby making up only a subset of all motor neuron axons innervating muscles controlling tail movements. That is, this TB+ sample did not innervate muscles originating from thoracic and lumbar vertebrae and acting on the tail via their long tendons (tail *extrinsic* muscles).[14] The TB labeled population of motor neurons was found bilaterally across multiple neurological levels (Figure 1A) and was positioned more medially in the ventral horn (265 ± 67 μm from the spinal cord midline) compared to FR+ or FE+ motor neurons (362 ± 98 μm from midline; Figure 1B). The medial localization of labeled cells is consistent with canonical neuroanatomical observations of motor neurons, validating the notion that we were observing motor neurons in the spinal cord.[19,20] In those animals in which two adjacent ventral roots were labeled, we observed a clear segmental delineation between FR+ and FE+ neurons, indicating that there was minimal spatial overlap in these motor neurons over adjacent neurological levels. In both this and the second experiment, we did not observe an appreciable difference in cross-sectional size of the cell somata across experimental groups when measured on a random sample of specimens, although volumetric analysis was not performed.

Double labeling of motor neurons—Figure 1 shows 94 FE+ motor neurons (Figure 1B; 1D) and 29 double labeled neurons (Figure 1C; 1F). Total cell counts for FR+ and FE+ motor neurons are depicted in Figure 1G. In the FR-labeled spinal cords (N=6), we observed 56 7 31 FR+ neurons and 21 ± 14 FR+TB+ (42 ± 16%). While FR labeling was originally performed in 8 animals, the tissue from two animals was poorly processed and therefore excluded from analysis. In the FE-labeled cords (N=4), we observed 75 ± 40 FE+ motor neurons and 22 ± 20 FE+TB+ neurons (29 ± 11%). Averaging cell count data across all animals, 36 ± 15% of FR+ or FE+ motor neurons were also labeled with TB. Once again, this percentage of double labeled cells represents the subset of motor neurons that form a single ventral root and contribute axons to the intrinsic tail muscles. For the purposes of experiments, these motor neurons give rise to axons that would be available for retrograde labeling at the second time-point in the axonal repair and regeneration component of this study. The upper bound of this last measure (51%) was thus used as a conservative correction factor to arrive at a more accurate value of the total number of potential motor neurons that might regenerate axons beyond the point of ventral root transection, as the remaining ventral root axons would have branched off to innervate extrinsic tail muscles and could not have been accounted for with retrograde labeling.

2: Axonal repair and regeneration

Retrograde labeling of regenerating axons—Representative micrographs of longitudinally cut spinal cords from treated animals are depicted in Figure 2. In panels C–F, TB+ motor neurons span the medial-lateral axis of the ventral horn, while the FR+ motor neurons labeled after axonal transection at the base of the tail reside more medially. Total counts of TB+ motor neurons were as follows: injury repair control group (NR: 139 ± 117),

acellular scaffold treatment (CL: 192 ± 137), and cellular scaffold treatment (CLSC: 194 ± 143; Figure 3A; p = 0.71). Comparison of double labeled cell counts, indicative of axonal regeneration, across groups was also not statistically significant (Figure 3A; NR: 23 ± 28;CL: 30 ± 25; CLSC: 62 ± 54; p = 0.16).

However, when the percentage of double labeled cells was averaged across animals and corrected for those axons that had branched off to extrinsic tail muscles prior to the secondary labeling point, this difference was significant (F = 4.78, p = 0.02; Figure 3B). Post hoc tests revealed that double labeling in the CLSC group (double labeled: 29.6 ± 20.2%; double labeled & corrected: 58.0 ± 39.6%) was significantly higher than that observed in the CL group (double labeled: 14.2 ± 8.2%; double labeled & corrected: 27.8 ± 16.0%; p = 0.02), though not significantly higher than that observed in the NR group (double labeled: 17.1 ± 9.3%; double labeled & corrected: 33.5 ± 18.2%; p = 0.10).

Discussion

Innervation of intrinsic and extrinsic tail muscles

The extrinsic tail muscles lie very close to the spine and are innervated by numerous neurological levels via several small nerve branches arising from spinal nerve rami and the caudales nerves.[14] Since the distal axonal projections of the sacrococcygeal ventral roots are so dispersed, it is difficult to assess axonal regeneration using "classical" serial retrograde labeling techniques, which are usually employed at two sites along a larger nerve with few branches.[16,17,21] We found that 36 ± 15% of rat sacrococcygeal ventral root axons innervate the intrinsic tail muscles, and used the upper bound of this percentage (51%) as a correction factor for employment of a modified version of this classical serial retrograde labeling technique. Presumably, a similar percentage of double labeled cells could be ascertained by applying the classical labeling approach with all of the distal projection. However, this is not feasible experimentally, as more nerve branches would have to be exposed and cut prior to the required survival period in which tracer transport occurs, causing unnecessary distress for the animal and a higher potential for spurious labeling secondary to unintended tracer spread.[22–24]

We also noted that "intrinsic-bound" cells were medially located in the ventral horn of the spinal cord. The longitudinal, columnar organization of motor neurons in the spinal cord was described almost 150 years ago,[19] though these columns were later subdivided into medial and lateral zones based on the muscle groups that they innervate.[20] Based on stimulation studies conducted by our group,[14] it is likely that motor neurons labeled with only FR or FE in the first experiment innervate the rat's extrinsic tail muscles.

In general, we observed lower cell counts with ventral root labeling as compared to our earlier reports of ventral root axon counts using neurofilament imaging, where an average of approximately 200 axons were observed in healthy S3, S4, and Co1 ventral roots.[13] This was likely due to both methodological differences in axonal tracer uptake versus immunohistochemical staining, and the use of conservative correction methods related to cell counting.

Strategies for repair of transected ventral roots

In peripheral nerve, microsurgical techniques facilitate the suturing of the connective tissue within the proximal and distal stumps, which optimizes the alignment of individual nerve fascicles. Compared to peripheral nerves, the fascicular pattern of nerve roots is less complex.[25] However, because nerve roots within the cauda equina lack an epineurium (i.e., the connective tissue around peripheral nerves),[26,27] directly repairing nerve roots with suture is difficult, if not impossible. Fibrin glue may be beneficial in cases where a limited gap between stumps exists.[6] However, high tensile forces have been shown to hinder neuronal regeneration,[28–30] and nerve root stumps are prone to retraction after transection. Alternatively, graft repair offers some degree of flexibility should a wider gap exist after injury or should an extensive amount of damaged neural tissue need to be surgically removed. While the autograft is still considered the best option, artificial grafts are improving,[31] and have the added advantage of being customizable for a specific nerve injury. Furthermore, by circumventing the need for an additional surgery, the use of artificial grafts does not put the patient at risk for neuroma formation at the harvest site, a phenomenon that occurs in approximately 10% of all patients undergoing autograft transfer.[32]

Schwann cell seeded collagen-laminin scaffolds

Numerous animal studies have successfully used collagen to repair peripheral nerves,[33–35] to the extent that FDA-approved collagen guidance channels are currently being used for repairing peripheral nerves in human patients with inter-stump gaps of up to 3 cm.[36–38] The combination of collagen I with laminin has been shown to result in improved neurite outgrowth in vitro[39,40] and *in vivo*,[41,42] although our results using acellular collagen-laminin grafts failed to show improved regeneration. In our study, however, Schwann cell seeded collagen scaffolds produced a much more robust regenerative effect; roughly two times that of acellular scaffolds. Schwann cells are major producers of neurotrophic factors [43,44] and have been shown to greatly promote axonal regeneration.[45–49] The success of Schwann cell seeded guidance channels has been frequently cited in studies involving injured peripheral nerves,[50–57] and one study in the primate cauda equina.[58] In this last study, implantation of autologous Schwann cells within an acrylonitrile vinyl chloride copolymer guidance channel yielded positive stimulus-evoked EMG results and regrowth across the injury site in three out of eight nerve roots.[58] However, guidance channel collapse was observed with equal frequency.[58] Indeed, surgical implantation constraints and channel collapse led us to abandon the guidance channel approach in the rat cauda equina in earlier experiments (data not shown). Using fibrin glue in conjunction with the scaffolds in the present study, we were also able to avoid the difficulties associated with surgically "threading" the nerve root ends into a guidance channel.

Limitations

This study has several limitations in addition to the potential tracer-associated issues discussed above. First, only anatomical assays were used to assess regeneration. Techniques that evaluate nerve function and animal behavior would be useful in future studies. Second, we did not assess the *accuracy* of regeneration. It is possible that some of the axons destined for intrinsic muscles of the tail did indeed regenerate but were misdirected to extrinsic

muscle targets prior to labeling with FR. Of course, this might be balanced by misdirected regeneration from extrinsic (originally) to intrinsic muscle targets. Third, some double labeling was observed in the NR group, which may reflect spontaneous regeneration without intervention in these animals. While the injury site gap was 3 mm for treated animals, nerve root stumps were reflected away from each other in the NR group, making growth into the distal stump unlikely, but not impossible. The number of double labeled cells in the spinal cords of NR animals was especially high after correcting for axons "lost" to extrinsic tail muscles prior to the site of secondary labeling. Again, this may be due to unintentional spread of TB in the intradural space.

Another limitation is that we could not identify the exact site of nerve root repair 9 weeks later, due to excessive scar tissue formation, hence we could not directly quantify axonal regeneration within repaired roots. Fluorescent graft substrates or other tissue labeling techniques may be used in future studies to facilitate identification of the injured area during microscopy.

This study utilized Fischer 344/DuCl rats to show the feasibility of the transplantation approach in a model lacking genetic heterogeneity. A similar transplant approach may someday be available for human patients through a Schwann cell "donor bank." Alternatively, assuming the continued development of more rapid in vitro methods of cell expansion, patients with cauda equina injury could be treated with artificial nerve grafts seeded with their own cells. This latter approach would be more conducive for maintaining the reactive Schwann cell phenotype that has been shown to facilitate axonal regeneration.[50,59,60]

Summary

In conclusion, our results demonstrate the feasibility of using Schwann cell seeded collagen-laminin scaffolds to repair transected ventral roots in a rat model of cauda equina injury. The restricted operational space around the rat cauda equina and small caliber of nerve roots (approximately 120–300 μm in diameter) should be taken into account when considering therapies for nerve root repair, as the larger operative space available in larger animal models and human patients affords the use of modified repair strategies, which could potentially result in a higher degree of regeneration. Future studies employing behavioral and electrophysiological assays to assess the degree of functional regeneration to muscle targets are needed to corroborate the findings from this study.

Supplementary Material

Refer to Web version on PubMed Central for supplementary material.

Acknowledgments

References

1. Thongtrangan I, Le H, Park J, Kim DH. Cauda equina syndrome in patients with low lumbar fractures. Neurosurgical Focus. 2004; 16:e6.

2. Kingwell SP, Noonan VK, Fisher CG, Graeb DA, Keynan O, Zhang H, et al. Relationship of neural axis level of injury to motor recovery and health-related quality of life in patients with a thoracolumbar spinal injury. J Bone Joint Surg Am. 2010; 92:1591–1599. [PubMed: 20595564]

3. Weber RV, Mackinnon SE. Bridging the neural gap. Clin Plast Surg. 2005; 32:605–616. viii. [PubMed: 16139631]

4. Zhang M, Yannas IV. Peripheral nerve regeneration. Adv Biochem Eng Biotechnol. 2005; 94:67–89. [PubMed: 15915869]

5. LeBlanc HJ, Gray LW, Kline DG. Stab wounds of the cauda equina. Case report. J Neurosurg. 1969; 31:683–685. [PubMed: 5359215]

6. Sun T, Liu Z, Liu S, Xu S. The clinical study of repairing cauda equina fibres with fibrin glue after lumbar fracture and dislocation. Spinal Cord. 2010; 48:633–637. [PubMed: 20142831]

7. Harrop JS, Hunt GE Jr, Vaccaro AR. Conus medullaris and cauda equina syndrome as a result of traumatic injuries: management principles. Neurosurgical Focus. 2004; 16:e4.

8. Pal D, Timothy J, Marks P. Penetrating spinal injury with wooden fragments causing cauda equina syndrome: case report and literature review. Eur Spine J. 2006; 15(Suppl 5):574–577. [PubMed: 16341555]

9. Piqueras C, Martinez-Lage JF, Almagro MJ, Ros De San Pedro J, Torres Tortosa P, Herrera A. Cauda equina-penetrating injury in a child. Case report. J Neurosurg. 2006; 104:279–281. [PubMed: 16619641]

10. Robertson DP, Simpson RK. Penetrating injuries restricted to the cauda equina: a retrospective review. Neurosurgery. 1992; 31:265–269. discussion 269–270. [PubMed: 1513432]

11. Robles LA. Transverse sacral fractures. Spine J. 2009; 9:60–69. [PubMed: 17981093]

12. Blaskiewicz DJ, Smirnov I, Cisu T, Deruisseau LR, Stelzner D, Calancie B. Cauda equina repair in the rat: 1. Stimulus-evoked EMG for identifying spinal nerves innervating intrinsic tail muscles. J Neurotrauma. 2009; 26:1405–1416. [PubMed: 19203211]

13. Mackenzie SJ, Smirnov I, Calancie B. Cauda Equina Repair in the Rat: Part 2. Time Course of Ventral Root Conduction Failure. J Neurotrauma. 2012; 29:1683–1690. [PubMed: 21361731]

14. Mackenzie SJ, Yi JL, Singla A, Russell TM, Calancie B. Innervation and function of rat tail muscles for modeling cauda equina injury and repair. Muscle Nerve. 2015; 52:94–102. [PubMed: 25346299]

15. Abercrombie M. Estimation of nuclear population from microtome sections. Anat Rec. 1946; 94:239–247. [PubMed: 21015608]

16. Al Majed AA, Brushart TM, Gordon T. Electrical stimulation accelerates and increases expression of BDNF and trkB mRNA in regenerating rat femoral motoneurons. Eur J Neurosci. 2000; 12:4381–4390. [PubMed: 11122348]

17. Bodine-Fowler SC, Meyer RS, Moskovitz A, Abrams R, Botte MJ. Inaccurate projection of rat soleus motoneurons: a comparison of nerve repair techniques. Muscle Nerve. 1997; 20:29–37. [PubMed: 8995580]

18. Brushart TM. Preferential motor reinnervation: a sequential double-labeling study. Restorative neurology and neuroscience. 1990; 1:281–287. [PubMed: 21551568]

19. Waldeyer, W. Das gorilla ruckenmark. Berlin: YEar

20. Sprague JM. A study of motor cell localization in the spinal cord of the rhesus monkey. Am J Anat. 1948; 82:1–26. [PubMed: 18919561]

21. Al-Majed AA, Neumann CM, Brushart TM, Gordon T. Brief electrical stimulation promotes the speed and accuracy of motor axonal regeneration. J Neurosci. 2000; 20:2602–2608. [PubMed: 10729340]

22. McNeill DL, Hoffman JM, Burden HW. Utilization of a polyethylene enclosure for nerve tracing studies in the rat ovary. J Neurosci Methods. 1986; 17:121–127. [PubMed: 3762221]

23. Ramsay H, House JR 3rd, Beattie JL, Moore JK. A simple technique for introducing anterograde and retrograde tracers into the vestibular and cochlear sensory organs. Acta Otolaryngol. 1996; 116:39–43. [PubMed: 8820348]

24. Haase P, Hrycyshyn AW. On the diffusion of horseradish peroxidase into muscles and the "spurious" labeling of motoneurons. Exp Neurol. 1986; 91:399–403. [PubMed: 3943582]

25. Suh YS, Chung K, Coggeshall RE. A study of axonal diameters and areas in lumbosacral roots and nerves in the rat. J Comp Neurol. 1984; 222:473–481. [PubMed: 6699214]

26. Beel JA, Stodieck LS, Luttges MW. Structural properties of spinal nerve roots: biomechanics. Exp Neurol. 1986; 91:30–40. [PubMed: 3940878]

27. Steer JM. Some observations on the fine structure of rat dorsal spinal nerve roots. J Anat. 1971; 109:467–485. [PubMed: 4949290]

28. Hentz VR, Rosen JM, Xiao SJ, McGill KC, Abraham G. The nerve gap dilemma: a comparison of nerves repaired end to end under tension with nerve grafts in a primate model. The Journal of hand surgery. 1993; 18:417–425. [PubMed: 8515008]

29. Sunderland IR, Brenner MJ, Singham J, Rickman SR, Hunter DA, Mackinnon SE. Effect of tension on nerve regeneration in rat sciatic nerve transection model. Ann Plast Surg. 2004; 53:382–387. [PubMed: 15385776]

30. Yi C, Dahlin LB. Impaired nerve regeneration and Schwann cell activation after repair with tension. Neuroreport. 2010; 21:958–962. [PubMed: 20729767]

31. Johnson EO, Soucacos PN. Nerve repair: experimental and clinical evaluation of biodegradable artificial nerve guides. Injury. 2008; 39(Suppl 3):S30–36. [PubMed: 18722612]

32. Ijpma F, Nicolai JP, Meek MF. Sural nerve donor-site morbidity: thirty-four years of follow-up. Ann Plast Surg. 2006; 57:391–395. [PubMed: 16998330]

33. Soller EC, Tzeranis DS, Miu K, So PT, Yannas IV. Common features of optimal collagen scaffolds that disrupt wound contraction and enhance regeneration both in peripheral nerves and in skin. Biomaterials. 2012; 33:4783–4791. [PubMed: 22483241]

34. Dornseifer U, Fichter AM, Leichtle S, Wilson A, Rupp A, Rodenacker K, et al. Peripheral nerve reconstruction with collagen tubes filled with denatured autologous muscle tissue in the rat model. Microsurgery. 2011; 31:632–641. [PubMed: 22072584]

35. Ding T, Luo ZJ, Zheng Y, Hu XY, Ye ZX. Rapid repair and regeneration of damaged rabbit sciatic nerves by tissue-engineered scaffold made from nano-silver and collagen type I. Injury. 2010; 41:522–527. [PubMed: 19524233]

36. Haug A, Bartels A, Kotas J, Kunesch E. Sensory recovery 1 year after bridging digital nerve defects with collagen tubes. The Journal of hand surgery. 2013; 38:90–97. [PubMed: 23261191]

37. Deal DN, Griffin JW, Hogan MV. Nerve conduits for nerve repair or reconstruction. J Am Acad Orthop Surg. 2012; 20:63–68. [PubMed: 22302443]

38. Taras JS, Jacoby SM, Lincoski CJ. Reconstruction of digital nerves with collagen conduits. The Journal of hand surgery. 2011; 36:1441–1446. [PubMed: 21816545]

39. Deister C, Aljabari S, Schmidt CE. Effects of collagen 1, fibronectin, laminin and hyaluronic acid concentration in multi-component gels on neurite extension. J Biomater Sci Polym Ed. 2007; 18:983–997. [PubMed: 17705994]

40. Swindle-Reilly KE, Papke JB, Kutosky HP, Throm A, Hammer JA, Harkins AB, et al. The impact of laminin on 3D neurite extension in collagen gels. Journal of neural engineering. 2012; 9:046007. [PubMed: 22736189]

41. Ding T, Lu WW, Zheng Y, Li Z, Pan H, Luo Z. Rapid repair of rat sciatic nerve injury using a nanosilver-embedded collagen scaffold coated with laminin and fibronectin. Regenerative medicine. 2011; 6:437–447. [PubMed: 21749202]

42. Cao J, Sun C, Zhao H, Xiao Z, Chen B, Gao J, et al. The use of laminin modified linear ordered collagen scaffolds loaded with laminin-binding ciliary neurotrophic factor for sciatic nerve regeneration in rats. Biomaterials. 2011; 32:3939–3948. [PubMed: 21397941]

43. Gordon T. The role of neurotrophic factors in nerve regeneration. Neurosurg Focus. 2009; 26:E3.

44. Hoke A, Redett R, Hameed H, Jari R, Zhou C, Li ZB, et al. Schwann cells express motor and sensory phenotypes that regulate axon regeneration. J Neurosci. 2006; 26:9646–9655. [PubMed: 16988035]

45. Xiong Y, Zhu JX, Fang ZY, Zeng CG, Zhang C, Qi GL, et al. Coseeded Schwann cells myelinate neurites from differentiated neural stem cells in neurotrophin-3-loaded PLGA carriers. International journal of nanomedicine. 2012; 7:1977–1989. [PubMed: 22619535]

46. Zavan B, Abatangelo G, Mazzoleni F, Bassetto F, Cortivo R, Vindigni V. New 3D hyaluronan-based scaffold for in vitro reconstruction of the rat sciatic nerve. Neurol Res. 2008; 30:190–196. [PubMed: 18397612]

47. Xie FK, Latalladi G, Kuffler DP. Neurotrophic influence of sciatic nerve-released factors on isolated adult motoneurons in vitro. J Peripher Nerv Syst. 1998; 3:37–46. [PubMed: 10959236]

48. Kuffler DP, Megwinoff O. Neurotrophic influence of denervated sciatic nerve on adult dorsal root ganglion neurons. J Neurobiol. 1994; 25:1267–1282. [PubMed: 7815058]

49. Sun XH, Che YQ, Tong XJ, Zhang LX, Feng Y, Xu AH, et al. Improving nerve regeneration of acellular nerve allografts seeded with SCs bridging the sciatic nerve defects of rat. Cell Mol Neurobiol. 2009; 29:347–353. [PubMed: 18987968]

50. Aszmann OC, Korak KJ, Luegmair M, Frey M. Bridging critical nerve defects through an acellular homograft seeded with autologous schwann cells obtained from a regeneration neuroma of the proximal stump. J Reconstr Microsurg. 2008; 24:151–158. [PubMed: 18438750]

51. Brown RE, Erdmann D, Lyons SF, Suchy H. The use of cultured Schwann cells in nerve repair in a rabbit hind-limb model. J Reconstr Microsurg. 1996; 12:149–152. [PubMed: 8726333]

52. Guenard V, Kleitman N, Morrissey T, Bunge RP, Aebischer P. Syngeneic Schwann cells derived from adult nerves seeded in semi-permeable guidance channels enhance peripheral nerve regeneration. J Neurosci. 1992; 12:3310–3320. [PubMed: 1527582]

53. Hadlock T, Sundback C, Hunter D, Cheney M, Vacanti JP. A polymer foam conduit seeded with Schwann cells promotes guided peripheral nerve regeneration. Tissue Eng. 2000; 6:119–127. [PubMed: 10941207]

54. Hood B, Levene HB, Levi AD. Transplantation of autologous Schwann cells for the repair of segmental peripheral nerve defects. Neurosurg Focus. 2009; 26:E4.

55. Levi AD, Sonntag VK, Dickman C, Mather J, Li RH, Cordoba SC, et al. The role of cultured Schwann cell grafts in the repair of gaps within the peripheral nervous system of primates. Exp Neurol. 1997; 143:25–36. [PubMed: 9000443]

56. Mosahebi A, Fuller P, Wiberg M, Terenghi G. Effect of allogeneic Schwann cell transplantation on peripheral nerve regeneration. Exp Neurol. 2002; 173:213–223. [PubMed: 11822885]

57. Radtke C, Akiyama Y, Lankford KL, Vogt PM, Krause DS, Kocsis JD. Integration of engrafted Schwann cells into injured peripheral nerve: axonal association and nodal formation on regenerated axons. Neurosci Lett. 2005; 387:85–89. [PubMed: 16084645]

58. Calancie B, Madsen PW, Wood P, Marcillo AE, Levi AD, Bunge RP. A guidance channel seeded with autologous Schwann cells for repair of cauda equina injury in a primate model. J Spinal Cord Med. 2009; 32:379–388. [PubMed: 19777858]

59. Strauch B, Rodriguez DM, Diaz J, Yu HL, Kaplan G, Weinstein DE. Autologous Schwann cells drive regeneration through a 6-cm autogenous venous nerve conduit. J Reconstr Microsurg. 2001; 17:589–595. discussion 596-587. [PubMed: 11740653]

60. Rodriguez FJ, Verdu E, Ceballos D, Navarro X. Nerve guides seeded with autologous Schwann cells improve nerve regeneration. Exp Neurol. 2000; 161:571–584. [PubMed: 10686077]
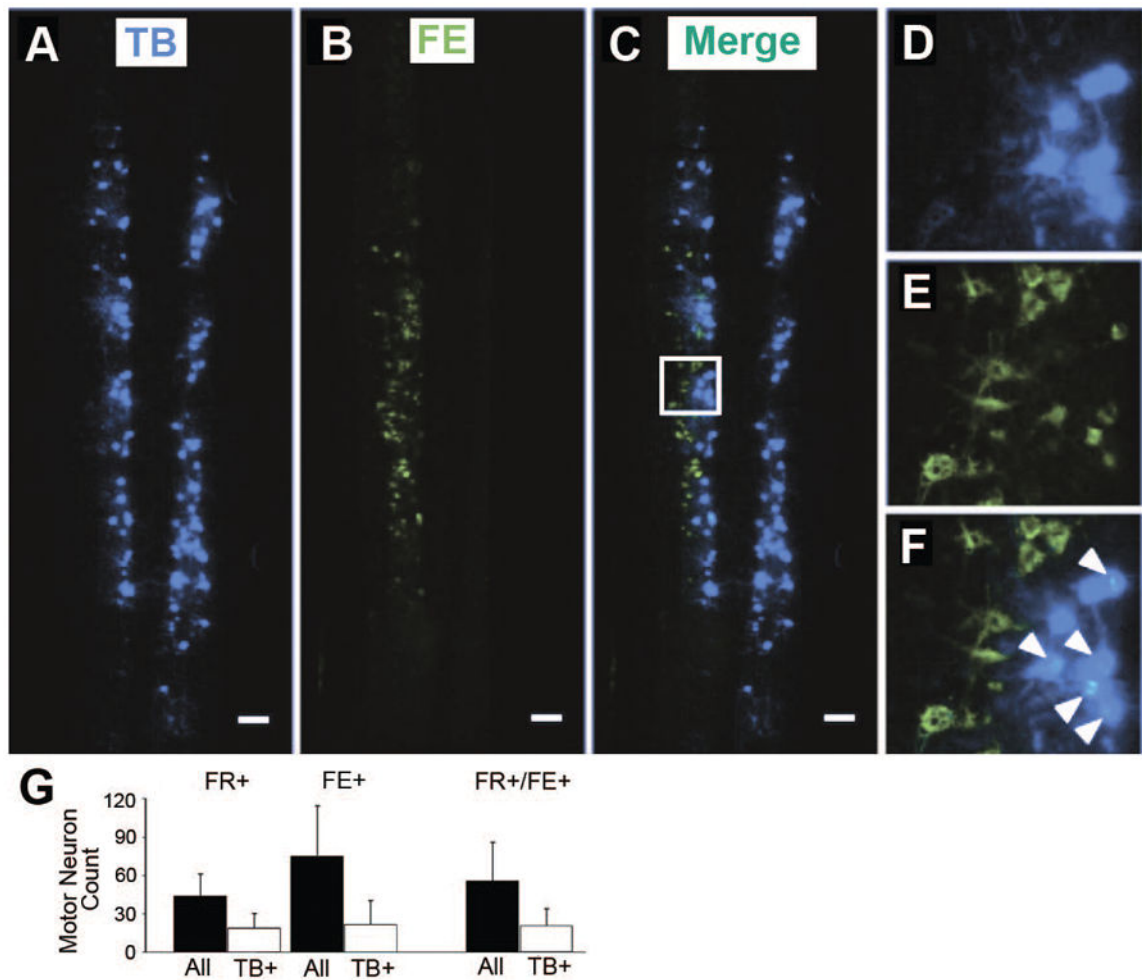
Figure 1. Longitudinal spinal cord section with True Blue, fluoro-emerald, and double labeled motor neurons (Experiment 1)

(A, D) Multiple motor neurons spanning multiple neurological levels were labeled bilaterally in the spinal cord after introduction of True Blue (TB) at the caudales nerves. (B, E) Fluoro-emerald (FE) labeling in the spinal cord following application of tracer at a single cut ventral root. (C, F) Double-labeled motor neurons (white arrows) comprised approximately one-third of the total FE-labeled population and were more medially located. Scale bars = 200 μm. (G) The four left-most bars represent averages for different tracers and tracer combinations. The two right-most bars represent merged averages. On average, 32% of motor neurons were double-labeled with either fluoro-ruby (FR+) and True Blue (TB+) or fluoro-emerald (FE+) and TB (36 ± 15% subject-weighted). Relatively fewer FR+ motor neurons were observed compared to FE+ neurons, though sample sizes were relatively small (FR-labeled spinal cords; N=6; FE-labeled spinal cords; N=4).
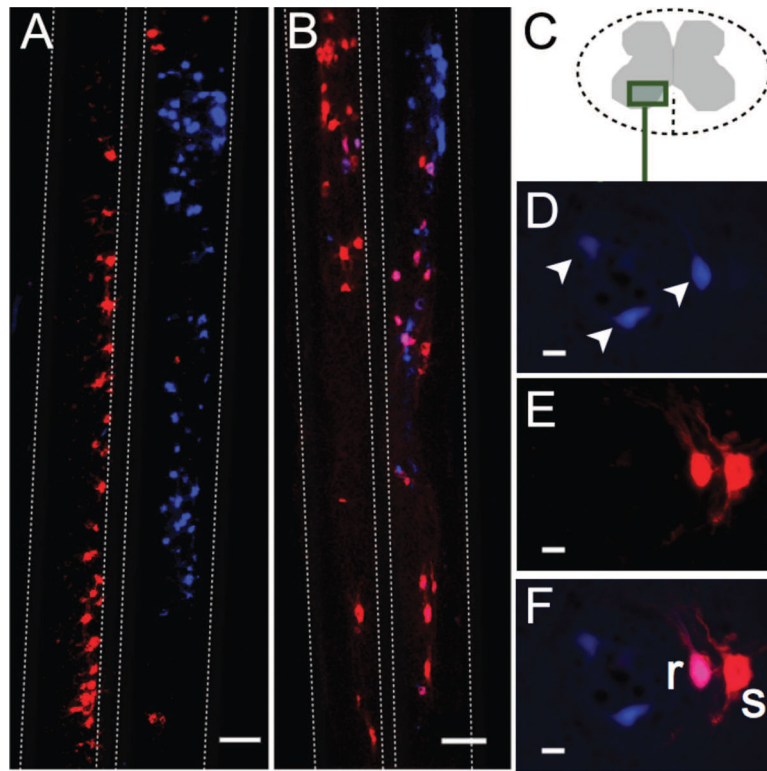
Figure 2. Longitudinal spinal cord sections with True Blue, fluoro-ruby, and double labeled motor neurons (Experiment 2)

A–B) Longitudinal spinal cord sections for (A) a CL animal and (B) a CLSC animal. Dashed lines demarcate gray matter-white matter boundaries. While the incidence of double labeling was 15.7% in the CL group, the image in (A) illustrates a complete lack of double labeling, which was occasionally observed. Scale bars = 200 μm. (D–F) Cross-sections at the S4 level from a rat in the CLSC group. (D) Injured (TB+; arrows), (E) spared (FR+ only; "s"), and regenerated (double-labeled FR+TB+; "r") motor neurons in the ventral horn (C). Scale bar = 20 μm.
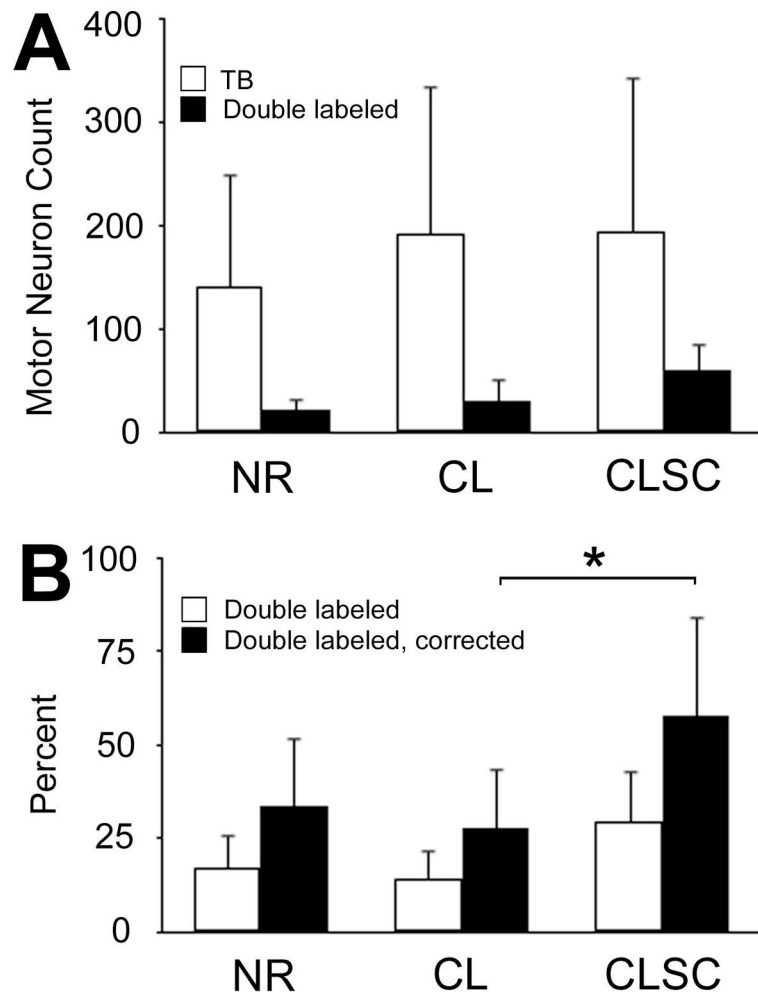
Figure 3. Quantitative comparison of double labeled motor neurons across groups (Experiment 2)

(A) True Blue (TB) labeling was slightly lower in no-repair (NR) animals and double labeling (DL) was slightly higher in animals treated with cellular scaffolds (CLSC), though these differences were not statistically significant. In general, motor neuron counts were variable across animals in all groups. (B) The percentage of double labeled cells was calculated for each group. These data were corrected to account for axons that had branched off to innervate extrinsic muscle targets prior to the point of secondary labeling. A group effect was noted for these corrected percentages with the CLSC group being significantly different from animals treated with unseeded collagen-laminin scaffolds (CL). Error bars reflect standard deviations across animals for each group. * p < 0.05.